

Experimental study of electron scale density fluctuation on HT-7 Tokamak

W.Y.Zhang*, Y.D.Li, S.Y.Lin, X.Gao, Y.X.Jie, X.D.Zhang, J. Li and the HT-7 Teams
Institute of Plasma Physics, Chinese Academy of Sciences, P.O.Box 1126, Hefei,
Anhui 230031, P.R.China
Contact: zhangwy@ipp.ac.cn

The behavior of the electron anomalous heat transport is a critical issue the reversed shear configurations in ignited plasma, where α -particle heating raises the electron temperature above the ion temperature. The trapped electron modes (TEM) driven turbulence and the electron temperature gradient (ETG) are possible candidates to explain the electron heat transport and the observed profile stiffness. Both of them have a threshold $(\nabla T_e / T_e)_c$, and above the threshold, the transport increases strongly, which tends to keep the T_e profile close to $(\nabla T_e / T_e)_c$. To understand the anomalous transport, turbulence measurements over a wide range in wavenumbers have been undertaken on a variety of fusion research devices [1-4]. For understanding the behavior of electron scale micro-instabilities in different plasma current profiles, the comparison between micro-instabilities of different wavenumber should be discussed in detail, which is one of the major purposes of this paper.

To investigate electron scale micro-instabilities, a CW CO₂ collective scattering system was installed on HT-7 tokamak. As shown in **Figure 1**, the chord is central, so the observed fluctuation wave-vector k is in the poloidal direction. Three independent channels with different scattering angles are used simultaneously to monitor density fluctuation in homodyne detection. The system can measure density fluctuation with $k_{\parallel} \rho_s = 1-4$ or TEM (trapped electron mode) and TEM/ETG (electron temperature gradient) scale.

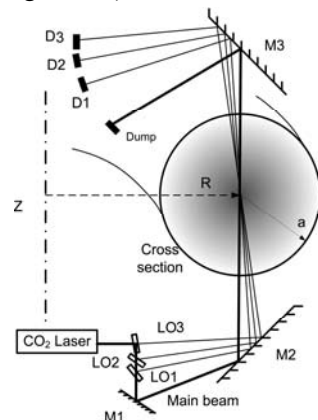


Fig.1: The schematic diagram of CW CO₂ collective scattering system on HT-7 tokamak.

The medium- and high- k domains density fluctuations were observed with increasing low hybrid power in lithium coating wall condition. It was found that a power threshold may exist. When the low hybrid power exceeded the threshold, the shape of frequency spectrum was not changed in channel $k_{\parallel} = 12 \text{ cm}^{-1}$ (**Figure 2a**), but the shape of frequency spectrum in channel $k_{\parallel} = 24 \text{ cm}^{-1}$ was obviously changed when low hybrid power exceeded 500kW (**Figure 2b**). The transition into the PLH>500kW phase may be attributable to the TEMs stabilization by the reversed current profile formed by LHCD (low hybrid current drive), whereas the steep ETG destabilized the small scale ETG modes [5, 6]. The typical time sequence of plasma current, LH power, loop voltage, central

line average density, H α and ECE signal of shot 106196(black) and 106197 (red) is plotted in **Figure 3**. LHCD was applied very early during the current ramp-up phase in every shot in order to create a non-monotonic q-profile. The low hybrid power, loop voltage, central line average density and plasma current of 106196 and 106197 is nearly the same, but H α show the core region confinement of 106196 is better than 106197. The ECE (channel 08 is in the core at about r/a~0.1) signal of 106196 makes a spontaneous transition into low hybrid enhanced performance mode [7]. The characteristic of the so-called hot-core low hybrid enhanced performance phase is the electron temperature profile peaks in the plasma core while the low hybrid power is constant. Abel inverted hard X-ray emission profiles of shot 106196 (**Figure 4**) could be used to reconstruct the total current profile in this non-inductive state sustained with low hybrid power because residual ohmic current was small. And the electron temperature profiles given by Thomson scattering system developed a steep gradient near r/a~0.4.

In another series shots of increasing low hybrid power in Boronization wall condition, the eruption in micro-instability appeared at a lower hybrid power larger than 475 kW with a plasma density of $\langle n_e \rangle \leq 2.1 \times 10^{19} \text{ m}^{-3}$ (**Figure 5 a, b**) was observed. When low hybrid power exceeded the threshold, the density fluctuation level enhanced and the frequency spectrum was broadened.

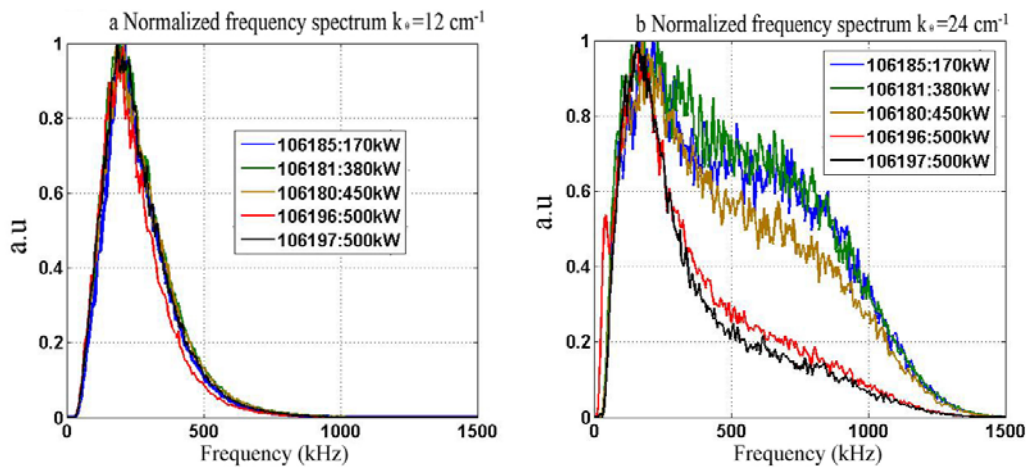


Fig.2 Frequency spectrum with different LH power. a: $k_{\perp} = 12 \text{ cm}^{-1}$; b: $k_{\perp} = 24 \text{ cm}^{-1}$.

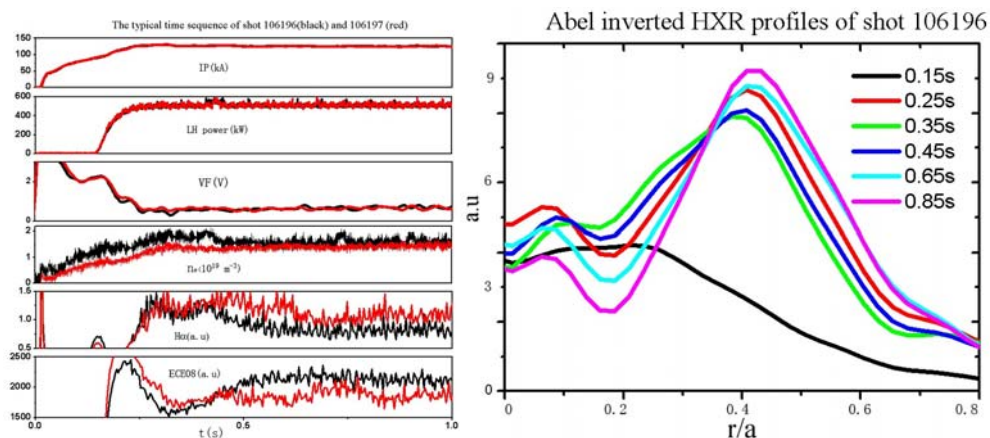


Fig.3: The typical time sequence of shot 106196(black) and 106197 (red).

Fig.4: Abel inverted HXR profiles of shot 106196.

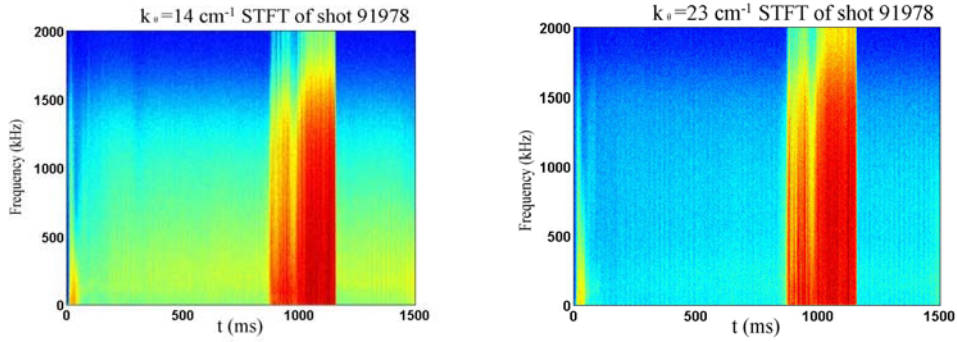


Fig.5 a: $k_0=14 \text{ cm}^{-1}$ STFT of shot 91978; b: $k_0=23 \text{ cm}^{-1}$ STFT of shot 91978.

The power spectrum of the density fluctuation (normalized to the squared density) is displayed in **Figure 6** and **Figure 7** as a function of wave-numbers (from $k_0=12 \text{ cm}^{-1}$ to $k_0=30 \text{ cm}^{-1}$) in different plasma parameters. In **Figure 6**, magnetic field $B_t=2\text{T}$, the power spectra follows power laws from $\sim b^{-3.15}$ to $\sim b^{-4.37}$. There is no obvious scale separation between middle and high k range, all the power spectra monotonically decrease. In **Figure 7**, when the magnetic field $B_t=1.8\text{T}$, the situation is opposite, all the power spectra are non-monotonic. Density spectra tend to be anisotropic at higher k and exhibit a flat region or modified power laws [8].

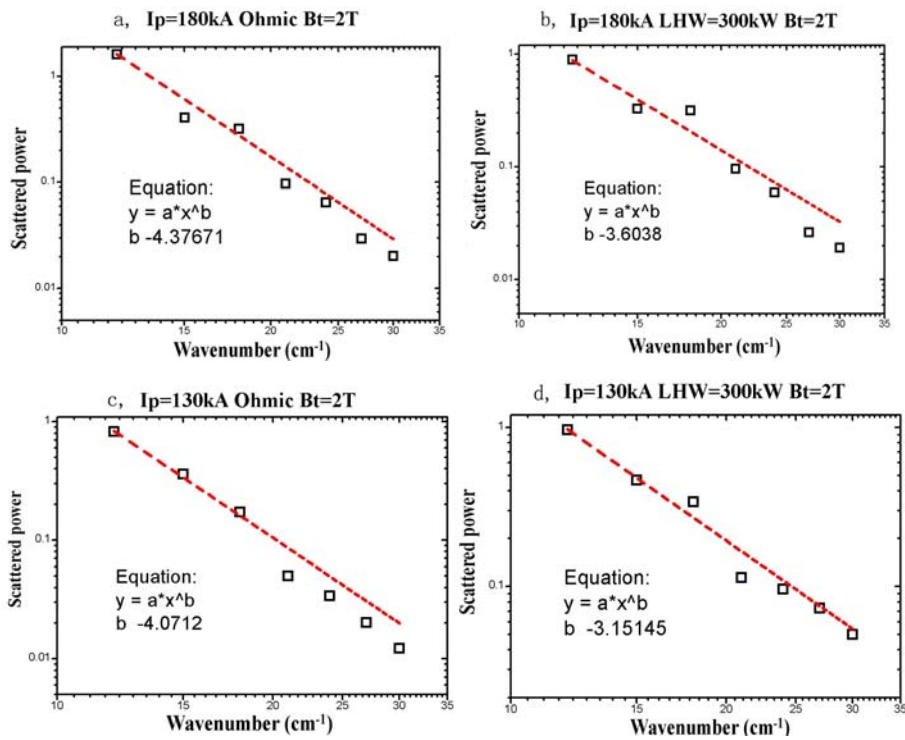


Fig.6 The power spectra were measured as a function of wave-numbers (logarithmic scales) with different plasma parameters. a: IP=180kA, ohmic, $B_t=2\text{T}$; b: IP=180kA, LHW=300kW, $B_t=2\text{T}$; c: IP=130kA, ohmic, $B_t=2\text{T}$; d: IP=130kA, LHW=300kW, $B_t=2\text{T}$.

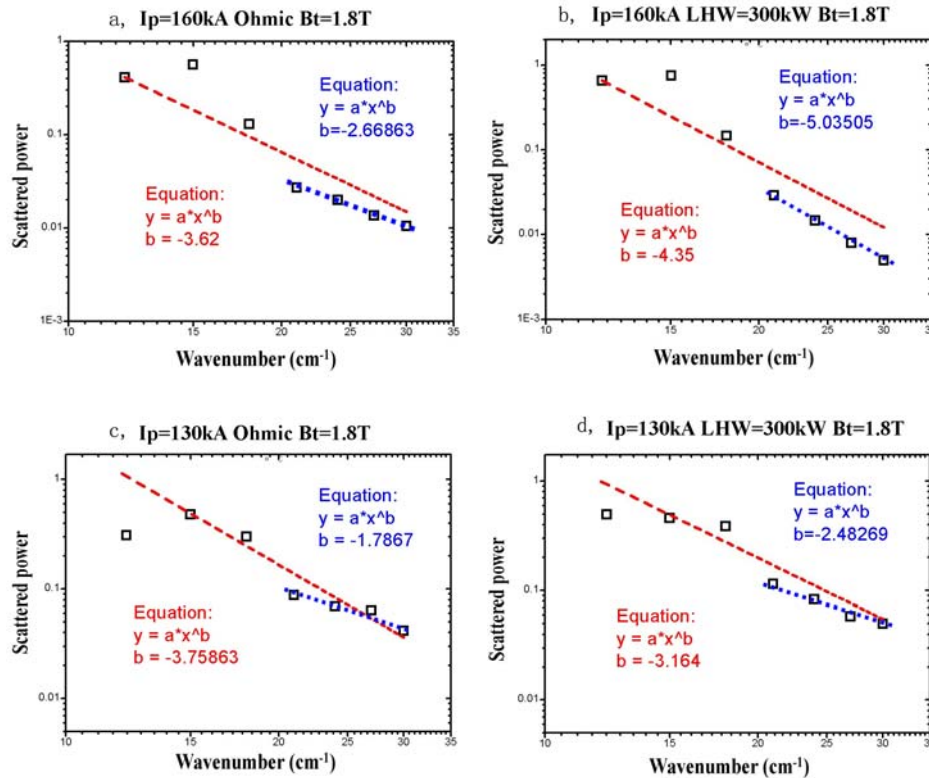


Fig.6 The power spectra were measured as a function of wave-numbers (logarithmic scales) with different plasma parameters. a: IP=160kA, ohmic, Bt=1.8T; b: IP=160kA, LHW=300kW, Bt=1.8T; c: IP=130kA, ohmic, Bt=1.8T; d: IP=130kA, LHW=300kW, Bt=1.8T.

References:

- [1] T.L. Rhodes, W.A. Peebles, X.V. Nguyen, Rev. Sci. Instrum. 77, 10E922 (2006)
- [2] E.Z. Gusakov, A.D. Gurchenko, A.B. Altukhov, Plasma Phys. Controlled Fusion 48 A371–6(2006)
- [3] P. Hennequin, R. Sabot, C Honor, G.T. Hoang, X. Garbet, Plasma Phys. Control. Fusion 46 B121 (2004)
- [4] E Mazzucato, D. R. Smith, R. E. Bell, S. M. Kaye, Phys. Rev. Lett. 101 075001 (2008)
- [5] Y .F. Baranov, X. Garbet, N. C. Hawkes, Plasma Phys. Control. Fusion 46 1181 (2004)
- [6] Li. Jiquan, Y. Kishimoto, Plasma Phys. Control. Fusion 44 A479 (2002)
- [7] X..Litaudon, Y.Peysson, T.Aniel, G.Huysmans, Plasma Phys. Control. Fusion 43 677-693 (2001)
- [8] T. Gorler, F. Jenko Phys. Rev. Lett. 100, 185002 (2008)